

XIN-MIN TANG

E-mail: tangxinmin@nuaa.edu.cn

YUN-XIANG HAN

College of Civil Aviation

Nanjing University of Aeronautics and Astronautics

29 Yudao St., Nanjing 210016, China

Science in Traffic and Transport

Original Scientific Paper

Accepted: Dec. 21, 2010

Approved: Mar. 14, 2012

4D TRAJECTORY ESTIMATION FOR AIR TRAFFIC CONTROL AUTOMATION SYSTEM BASED ON HYBRID SYSTEM THEORY

SUMMARY

To resolve the problem of future airspace management under great traffic flow and high density condition, 4D trajectory estimation has become one of the core technologies of the next new generation air traffic control automation system. According to the flight profile and the dynamics models of different aircraft types under different flight conditions, a hybrid system model that switches the aircraft from one flight stage to another with aircraft state changing continuously in one state is constructed. Additionally, air temperature and wind speed are used to modify aircraft true airspeed as well as ground speed, and the hybrid system evolution simulation is used to estimate aircraft 4D trajectory. The case study proves that 4D trajectory estimated through hybrid system model can image the flight dynamic states of aircraft and satisfy the needs of the planned flight altitude profile.

KEY WORDS

air traffic management, 4D trajectory estimation, hybrid system model, aircraft dynamic model

1. INTRODUCTION

With the rapid development of the global air transport and the increasing congestion of limited airspace resources, still using the air traffic control mechanism in a combination with advanced flight plan for the complex air traffic flow shows its backwardness. There is no exact separation for aircraft in the flight plan, which may lead to air traffic congestion and reduce airspace safety. The air traffic control automation system based on the flight plan cannot estimate the flight trajectory of the altitude profile, which results in its poor conflict resolution. Air traffic control work still focuses on maintaining safe separation for individual aircraft, and as the result, it is difficult to rise to the strategic management for the traffic flow.

Therefore, Europe and the USA implemented their next-generation air traffic management system, called Single European Sky ATM Research (SESAR) and Next

Generation Air Transportation System (NGATS), respectively [1-2], whose destination is to improve air traffic control service quality. One of their core technologies is 4D trajectory-based operation, which changes the existing flight plan and air traffic control into a new mechanism in the high-density airspace [1]. 4D trajectory accurately describes the location (longitude, latitude and altitude) and time of the aircraft, so that 4D trajectory-based operation is to control the arrival time windows of the aircraft arrived to an airway point [4]. Generally, 4D trajectory-based operation is an effective means for airspace management with high density and close separation, and it can significantly reduce the uncertainty of aircraft trajectory and improve the safety and operation efficiency of the airspace and airports [5].

4D flight trajectory estimation and generation have been widely investigated during the last decade. The research method can be divided into two categories. The first one is the non-parametric method such as Kalman filter and Neural network estimation algorithm. Wu proposed an estimation model based on data mining. In his research, aircraft historical trajectory data were analyzed to obtain the aircraft location in each sampling period [6]. This method operates well through the historical flight trajectory under normal circumstances, but it requires a lot of historical sampling data, and if disturbance such as air traffic control, meteorological environment changing occurs, this method cannot make the appropriate adjustments. The second one is Building aircraft model for simulation. R. Slatery proposed trajectory generation algorithm for radar control automation system. In this algorithm, the flight trace is connected through the designated points with straight lines or arcs, the vertical flight profile is divided into a series of flight segments and the second-order Runge-Kutta method is used to generate the trajectory [7]. Richard and Lee studied 4D trajectory estimation in the stage of take-off, climb and approaching [8, 9]. Wu studied the solution and synthesis for vertical

flight profiles [10]. Wang proposed the concept of basic flight model, constructed horizontal trajectory, altitude profile and speed profile for each basic flight model. A whole 4D trajectory was obtained by combining the flight states of characteristic points of trajectory, including location, altitude, speed, and heading [11]. Chester proposed a method using climbing time table from the flight performance manual to get aerodynamic models and the dynamic equation of aircraft for flight trajectory estimation [12]. Generally, for the reason of changing meteorological factors and the performance difference caused by different aircraft types, the accuracy of trajectory estimation is not ideal.

This paper is structured as follows: in Section 2, based on force analysis, a dynamic model for aircraft is built. In Section 3, according to the division of the aircraft flight profile and the dynamic model in different flight conditions, a hybrid system model that switches the aircraft from one flight stage to another with aircraft state changing continuously in one state is constructed. In Section 4, the meteorological factors are introduced to modify aircraft true airspeed and ground speed, and aircraft state is calculated step by step to generate aircraft 4D trajectory. In Section 5, an example is illustrated to describe how to estimate aircraft trajectory using the hybrid system model.

2. CONTINUOUS DYNAMIC MODELS OF AIRCRAFT

2.1 Force analysis for aircraft

As shown in *Figure 1*, the force acting on an aircraft includes engine thrust T_{HR} , drag D_{RG} , lift L_{FT} , the weight of the aircraft W during flight, and the forces change dynamically along with the switching of the flight state of the aircraft [13].

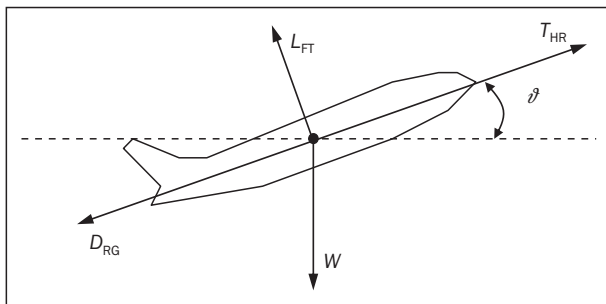


Figure 1 - Forces acting on aircraft in flight

First of all, the maximum thrust of engine during climb after take-off, cruise and descent stage should be considered separately.

Under the international standard atmospheric conditions (ISA), the turbine jet engine's maximum climb thrust may be expressed [13]:

$$(T_{max}^{climb})_{ISA} = C_{Tc,1} \cdot \left(1 - \frac{h_p}{C_{Tc,2}} + C_{Tc,3} \cdot h_p^2\right) \quad (1)$$

where h_p is geopotential pressure altitude. When differential value between the atmosphere temperature at the aircraft location t_{LOC} and international standard atmospheric temperature t_{ISA} is Δt , the maximum climb thrust of the engine is corrected [13]:

$$T_{max}^{climb} = (T_{max}^{climb})_{ISA} \cdot [1 - C_{Tc,5} \cdot (\Delta t - C_{Tc,4})] \quad (2)$$

In formula (1) and formula (2), $C_{Tc,1}$, $C_{Tc,2}$, $C_{Tc,3}$, $C_{Tc,4}$, $C_{Tc,5}$ are jet engine's thrust coefficients, whose dimension are N, ft, $1/ft^2$, $^{\circ}C$, $1/^{\circ}C$, respectively.

However, to extend the turbine jet engine's life and reduce the cost of the aircraft during climb, reduced climb power rather than maximum climb power is introduced. The reduced rate of the power used depends on the actual thrust profile in the flight manual [13].

$$C_{Pow}^{reduce} = 1 - C_{reduce} \cdot \frac{m_{max} - m_{act}}{m_{max} - m_{min}} \quad (3)$$

where C_{reduce} is the reduced power coefficients and depends on h_p and maximum altitude h_{max} , if h_p is less than $0.8 \cdot h_{max}$, then the value $C_{reduce} = 0.15$, else the value $C_{reduce} = 0$. Notations m_{max} , m_{min} and m_{act} represent maximal, minimal and actual aircraft mass respectively.

The maximum cruise thrust is proportional to the maximum climb thrust by constant C_{Tcr} :

$$T_{max}^{cruise} = C_{Tcr} \cdot T_{max}^{climb} \quad (4)$$

Maximum descent thrust is proportional to the maximum climb thrust by the coefficient depending on the flight altitude and configuration of the aircraft [13].

$$T_{max}^{descent} = \begin{cases} C_{Tdes}^{high} \cdot T_{max}^{climb}, h_p > h_p^{descent} \\ C_{Tdes}^{low} \cdot T_{max}^{climb}, h_p < h_p^{descent}, \text{cruise} \\ C_{Tdes}^{approach} \cdot T_{max}^{climb}, h_p < h_p^{descent}, \text{approach} \\ C_{Tdes}^{landing} \cdot T_{max}^{climb}, h_p < h_p^{descent}, \text{landing} \end{cases} \quad (5)$$

where C_{Tdes}^{high} , C_{Tdes}^{low} , $C_{Tdes}^{approach}$, $C_{Tdes}^{landing}$ are correction factors used for high and low altitudes, approach and landing configurations.

Second, according to *Figure 1*, to balance the force from the direction of lift, the lift of aircraft L_{FT} during flight should meet:

$$L_{FT} = \frac{C_L}{2} \rho \cdot v_{TAS}^2 \cdot S = W \cdot \cos \gamma \quad (6)$$

where ρ is air density, and v_{TAS} is true airspeed, and S is reference wing surface area, then the lift coefficient C_L is explained below:

$$C_L = \frac{2W \cdot \cos \gamma}{\rho \cdot v_{TAS}^2 \cdot S} \quad (7)$$

Under normal circumstances, the drag coefficient C_D is a function of the lift coefficient C_L [13]:

$$C_D = \begin{cases} C_{D0}^{cruise} + C_{D2}^{cruise} \cdot (C_L)^2, \text{cruise} \\ C_{D0}^{approach} + C_{D2}^{approach} \cdot (C_L)^2, \text{approach} \\ C_{D0}^{landing} + C_{D0}^{gear} + C_{D2}^{landing} \cdot (C_L)^2, \text{landing} \end{cases} \quad (8)$$

where C_{D0}^{cruise} , C_{D2}^{cruise} , $C_{D0}^{approach}$, $C_{D2}^{approach}$, $C_{D0}^{landing}$, $C_{D2}^{landing}$ are coefficients for the specification of drag in the stage of cruise, approach and landing respectively, and C_{D0}^{gear} represents drag increase due to the landing gear.

The drag can be described as follows:

$$D_{RG} = \frac{C_D}{2} \rho \cdot v_{TAS}^2 \cdot S \quad (10)$$

Finally, with the fuel consumption of the aircraft during flight, its weight W will decrease. For turbine jet engine, the fuel flow depends on true airspeed, flight altitude and engine thrust. Assume that the fuel flow is expressed by f_{ENG} for all flight stages.

The thrust specific fuel consumption ζ is specified as a function of true airspeed v_{TAS} [13]:

$$\zeta = C_{f1} \cdot \left(1 + \frac{v_{TAS}}{C_{f2}}\right) \quad (11)$$

where C_{f1} and C_{f2} are fuel consumption coefficients, whose dimensions are kg/(min·kN) and kt respectively. In a general way, the fuel flow per unit time f_{nom} (kg/min) during climb stage is calculated:

$$f_{nom} = \zeta \cdot T_{HR} \quad (12)$$

Fuel consumption per unit time f_{min} is specified as function of flight altitude [13]:

$$f_{min} = C_{f3} \cdot \left(1 - \frac{h_p}{C_{f4}}\right) \quad (13)$$

where C_{f3} and C_{f4} are descent fuel consumption coefficients, whose dimensions are kg/min and ft respectively. The fuel flow per unit time during approaching and landing stage is calculated [13]:

$$f_{app/landing} = \max\{f_{nom}, f_{min}\} \quad (14)$$

Fuel consumption is specified as a function of engine thrust during cruise stage [13]:

$$f_{cruise} = \zeta \cdot T_{HR} \cdot C_{fcr} \quad (15)$$

where C_{fcr} is cruise fuel consumption correction coefficient, which is dimensionless.

2.2 Aircraft dynamic model

Based on the total energy model, the relation between external forces acting on the aircraft and the change rate of aircraft energy can be expressed as follows:

$$(T_{HR} - D_{RG}) \cdot v_{TAS} = W \frac{dh}{d\tau} + \frac{W}{g} \cdot v_{TAS} \frac{dv_{TAS}}{d\tau} \quad (16)$$

where h is geodetic altitude and represents the aircraft distance above or below the ellipsoid as measured along a line that passes through the aircraft and is normal to the surface of the WGS-84 (World Geodetic System 1984) ellipsoid, $g = 9.80665 \text{ m/s}^2$ represents gravitational acceleration.

According to the formula above, the known aircraft thrust T_{HR} , the true airspeed v_{TAS} , the rate of climb and descent are calculated:

$$\frac{dh}{d\tau} = \frac{(T_{HR} - D_{RG}) \cdot v_{TAS}}{W} \left(1 + \frac{v_{TAS}}{g} \frac{dv_{TAS}}{dh}\right)^{-1} \quad (17)$$

Now define a_f as the acceleration factor during climb and descent, calculated by the following formula:

$$a_f = \frac{v_{TAS}}{g} \frac{dv_{TAS}}{dh} = \frac{k}{2} M^2 \cdot \left(1 - \lambda \frac{R}{g}\right) \quad (18)$$

where $k = 1.4$ is the gas adiabatic exponent, and $R = 287.06$ is the real gas constant for air, whose dimension is $\text{m}^2/(\text{K}\cdot\text{s}^2)$, M is Mach number. The attenuation rate λ of standard atmosphere changes along with the altitude in the troposphere and the stratosphere:

- 1) when $h_p < 36,089$ ft, the value $\lambda = -0.0065$. If $v_{cas} = \text{const.}$, then calibrated airspeed remains unchanged, and $a_f = 0.56682M^2$. If $M = \text{const.}$, i.e. Mach number remains unchanged, then $a_f = -0.133318M^2$.
- 2) when $h_p > 36,089$ ft, the value $\lambda = 0$. If the calibrated airspeed remains unchanged, then $a_f = 0.7M^2$. If Mach number remains unchanged, then $a_f = 0$.

Therefore, the rate of climb and descent can be expressed as:

$$\frac{dh}{d\tau} = \frac{(T_{HR} - D_{RG}) \cdot v_{TAS}}{W} (1 + a_f)^{-1} \quad (19)$$

Under the reduced climb power condition, the rate of climb and descent is:

$$\frac{dh}{d\tau} = \frac{(T_{max}^{climb} - D_{RG}) \cdot C_{pow}^{red} \cdot v_{TAS}}{W} \cdot (1 + a_f)^{-1} \quad (20)$$

If the pressure altitude is adopted to express aircraft flight altitude, and the temperature differential value between atmosphere temperature t_{LOC} and international standard atmospheric temperature t_{ISA} is Δt , then the rate of climb and descent v_H expressed by pressure altitude can be revised as:

$$v_H = \frac{dh_p}{d\tau} = \frac{t_{LOC} - \Delta t}{t_{LOC}} \cdot \frac{dh}{d\tau} \quad (21)$$

3. ENTIRE FLIGHT PROFILE HYBRID SYSTEM MODEL

3.1 Aircraft entire flight profile

As illustrated in Figure 2, the aircraft flight profile is mainly divided into three phases: climb, cruise and descent. Each flight phase is subdivided into several stages and speed parameters for each stage are defined as follows:

- 1) climb phase: take-off from the ground and accelerating to calibrated speed v_1^{climb} in stage *a*, climbing from 1,500 ft to 10,000 ft and remaining calibrated airspeed unchanged in stage *b*, accelerating to climb calibrated airspeed v_2^{climb} at altitude 10,000 ft in stage *c*, climbing to the cruise altitude and remaining Mach number M^{climb} unchanged in stage *d*.

- 2) cruise phase: accelerating to cruising Mach number M^{cruise} in stage e, cruising and remaining Mach number M^{cruise} unchanged in stage f, and maintaining the altitude to the descent point.
- 3) descent phase: maintaining the calibrated airspeed and descent to 10,000 ft in stage g, decelerating to a calibrated speed $v_1^{descent}$ and remaining the altitude unchanged in stage h, descending to 1,500 ft and remaining calibrated airspeed unchanged in stage i, decelerating to $v_1^{landing}$ and landing in stage j.

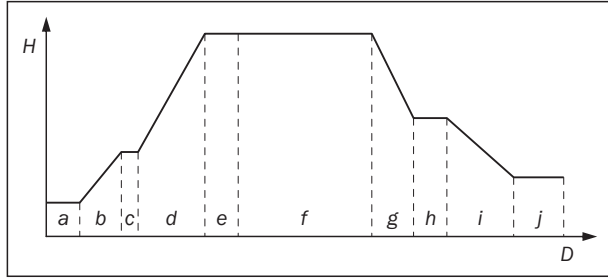


Figure 2 - Division of aircraft flight profile

3.2 Entire flight profile hybrid model

The profile of aircraft flying along the trajectory can be described by the continuous changing of physical state (including weight W , range D and altitude H) in one flight stage and switching from one stage to another dynamically. To describe the switching process, an aircraft flight stage transition model is established:

Definition 1 The Petri net $N = (P, T, \mathbf{Pre}, \mathbf{Post}, \mathbf{m})$ is an aircraft flight stage transition model in which P is a place set that represents flight stages, T a transition set that represents transition points of flight state parameters (including indicated speed, altitude, and configuration) in vertical profile, \mathbf{Pre} (or \mathbf{Post}) is a connective matrix that represents the connection between flight stages (or transition points) and transition points (or flight stages) and, finally, $\mathbf{m}: P \rightarrow Z$ is a

marking vector that represents the flight stage where the aircraft locates.

The process aircraft switches from the previous flight stage to the next one are discrete, while the procedure of aircraft evolving in a single stage is continuous. Therefore, the aircraft entire flight profile model is a typical hybrid system model.

Definition 2 The hybrid Petri net with continuous variable $HPN = (N, \mathbf{s}, \mathbf{e}, E)$ is aircraft entire flight profile model, where N is the aircraft flight stage transition model defined above. The aircraft state vector $\mathbf{s} = (W, D, H)$ belongs to continuous space, where $W: P \rightarrow R^+$ represents aircraft weight in the given flight stage, $D: P \rightarrow R^+$ represents accumulative flight range from departure airport and $H: P \rightarrow [FL_{min}, FL_{max}]$ represents the standard pressure altitude. Aircraft dynamic behaviour is noted by $\mathbf{e} = (V, A)$, where $V: T \rightarrow [v_{min}, v_{max}]$ represents airspeed to the next transition point (calibrated airspeed or Mach number), and $A: T \rightarrow [a_{min}, a_{max}]$ represents acceleration. The transition firing finish characteristic function is $E: T \rightarrow C$, where $C = \{H = h_i, D = d_i, V = v_i\}$ represents transition firing finish condition set.

Figure 3 shows the aircraft entire flight profile hybrid system model, in which an aircraft locates in the initial stage m_0 with state \mathbf{s}_0 and dynamic behaviour \mathbf{e} , where W_0 is the take-off weight, h_{ele}^{org} is departure airport elevation.

Additionally, to describe dynamic behaviour of the aircraft accurately, the transition enabling and firing condition is described as follows. For all places before transition t , i.e., $\forall p \in \cdot t$, if $\mathbf{m}(p) > 0$ then transition t is enabled and begins to fire. Assume the transition cumulative firing time is $\Delta\tau$, which will lead to change in its dynamic behavioural changed into $\mathbf{e}' = [V'(t), A'(t)]$, where:

$$V'(t) = V(t) + \int_0^{\Delta\tau} A(t) d\tau \quad (22)$$

The flight state vector corresponding to place p is changed into $\mathbf{s}' = [W', H', D']$, where aircraft weight is:

$$W'(p) = W(p) - \int_0^{\Delta\tau} \dot{W}_{ENG}(\tau) d\tau \quad (23)$$

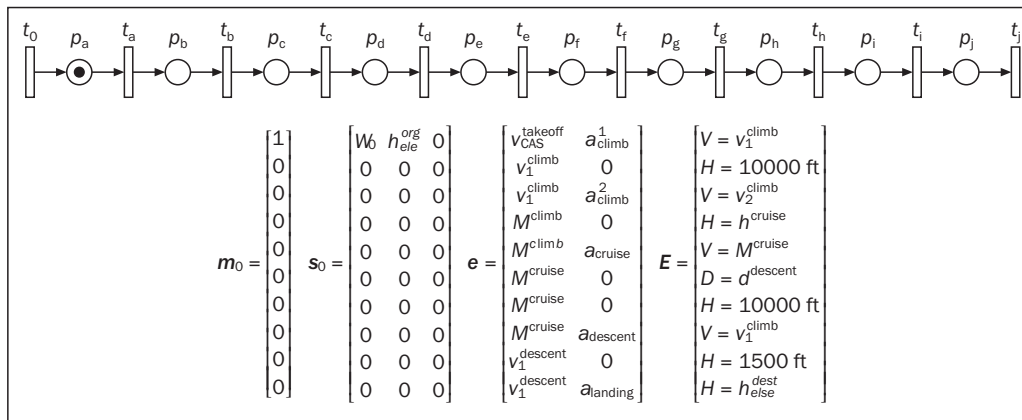


Figure 3 -Aircraft entire flight profile hybrid system model

The altitude from departure airport depends on the aircraft rate of climb and descent v_H expressed by pressure altitude:

$$H'(p) = H(p) + \int_0^{\Delta\tau} v_H(\tau) d\tau \quad (24)$$

The range from departure airport depends on the aircraft ground speed v_{GS} :

$$D'(p) = D(p) + \int_0^{\Delta\tau} v_{GS}(\tau) d\tau \quad (25)$$

The cumulative firing time $\Delta\tau$ of transition t depends on transition firing finish characteristic condition $E(t)$. If $E(t)$ is satisfied, then firing of transition t will finish, and location of aircraft will become m' :

$$m'(p) = \begin{cases} m(p) + 1, p \in t' \\ m(p) - 1, p \in \bar{t} \\ m(p), p \notin t' \wedge p \notin \bar{t} \end{cases} \quad (26)$$

This means that for all places before transition t , i.e, for all $p \in \bar{t}$, their tokens should be removed, and for all places after transition t , i.e, for all $p \in t'$, their tokens should be added. Otherwise, the aircraft will still locate in its original flight stage. Then let $\tau = \tau + \Delta\tau$ and recalculate continuous state vector and discrete states of aircraft using formula (22)~(26)

4. 4D TRAJECTORY ESTIMATION WITH METEOROLOGICAL FACTORS

To improve the accuracy of the aircraft trajectory estimation, meteorological environmental factors (including wind speed and direction, air temperature) should be considered.

4.1 Kinematic model considering meteorological factors

Generally speaking, the true airspeed will change along with the changing of flight altitude and air temperature. If $h_p < 36,089$ ft, the international standard atmospheric temperature $t_{ISA} = 288.15 - 1.9812 \cdot h/100$ K, else if $h_p > 36,089$ ft, $t_{ISA} = 216.65$ K. Assume that the air temperature of aircraft location is $t_{LOC} = t_{ISA} + \Delta t$, the mapping from calibrated airspeed v_{CAS} and Mach number M considering altitude, air temperature to true airspeed is built as follows.

1) sound speed v_A for remaining calibrated airspeed unchanged flight:

$$v_A = 661.5 \times \left(\frac{t_{LOC}}{t_{MSL}} \right)^{0.5} \quad (27)$$

where $t_{MSL} = 288.15$ K represents mean sea level standard atmospheric temperature, and the true airspeed is calculated as a function of the calibrated airspeed v_{CAS} :

$$v_{TAS} = 1,479.1 \times \left(\frac{t_{LOC}}{t_{MSL}} \left[\left(1 + \frac{\eta}{\delta} \right)^{1/3.5} - 1 \right] \right)^{0.5} \quad (28)$$

where symbol η is explained below:

$$\eta = \left[1 + 0.2 \times \left(\frac{v_{CAS}}{661.5} \right)^2 \right]^{3.5} - 1 \quad (29)$$

where $\delta = p/p_0$, and p represents actual pressure, p_0 represents standard pressure at MSL. δ can be calculated as a function of the geopotential pressure altitude h_p .

$$\delta = \begin{cases} (1 - 6.87559 \times 10^{-6} \times h_p)^{5.25588}, h_p \leq 36089 \text{ ft} \\ 0.2233609 \times \text{EXP}\left(\frac{30689 - h_p}{20805.8}\right), h_p > 36089 \text{ ft} \end{cases} \quad (30)$$

2) true airspeed v_{TAS} for remaining Mach number unchanged flight:

$$v_{TAS} = M \cdot v_A \quad (31)$$

Given the crossing angle α between the wind direction and flight airway, wind speed v_{WS} at aircraft location through meteorological prediction, the aircraft ground speed v_{GS} can be calculated according to relative motion equation:

$$v_{GS} = v_{TAS} + v_{WS} \cdot \cos \alpha \quad (32)$$

Finally, the rate of climb and descent v_H and ground speed v_{GS} can be established as follows:

$$\begin{cases} v_H = \kappa(v_{CAS}, M, h, t_{LOC}) \\ v_{GS} = \lambda(v_{CAS}, M, h, t_{LOC}, v_{WS}, \alpha) \end{cases} \quad (33)$$

4.2 4D trajectory estimation based on simulation

Assume that the moment the hybrid system enters the current marking m_0 is τ_0 . This means there exists $p \in P$, $m_0(p) = 1$ and the aircraft state is $s = [w_i, h_i, d_i]$ with dynamic behaviour $e = [v_i, a_i]$. Before transition firing finish condition is satisfied at the moment $\tau_0 + \Delta\tau$, and if $\Delta\tau$ is small enough, the change value of calibrated speed is represented as:

$$\Delta v_{CAS} = a_i \cdot \Delta\tau \quad (34)$$

The change of aircraft state is $\Delta s = [\Delta w, \Delta h, \Delta d]$:

$$\begin{cases} \Delta w = \bar{v}_{ENG} \cdot \Delta\tau \\ \Delta h = \bar{v}_H \cdot \Delta\tau \\ \Delta d = \bar{v}_{GS} \cdot \Delta\tau \end{cases} \quad (35)$$

where \bar{v}_H is mean rate of climb and descent, and \bar{v}_{GS} is mean ground speed of aircraft in the period of $\Delta\tau$:

$$\begin{cases} \bar{v}_H = \frac{\kappa(v_{CAS}, \dots) + \kappa(v_{CAS} + \Delta v_{CAS}, \dots)}{2} \\ \bar{v}_{GS} = \frac{\lambda(v_{CAS}, \dots) + \lambda(v_{CAS} + \Delta v_{CAS}, \dots)}{2} \end{cases} \quad (36)$$

Whereafter, subdividing time can calculate aircraft flight range and altitude step by step in a certain flight stage. Figure 4 is the curve describing the altitude and range changing with time, which is expressed as mapping function $h(\tau)$ and $d(\tau)$ respectively.

Finally, combining the required flight airway model, which is the mapping from longitude x to latitude y ,

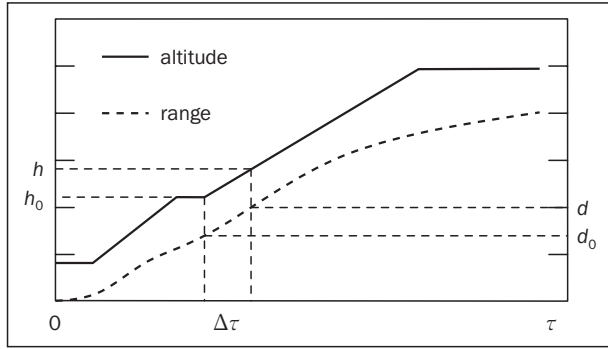


Figure 4 - Aircraft flight range and altitude curve

noted as $\pi: x \rightarrow y(x)$, longitude x of aircraft at moment $\tau = \tau_0 + \Delta\tau$ can be estimated through equation listed as follows:

$$d(\tau) = \int_{x_0}^x \frac{y(x)}{\sqrt{1 + (y'(x))^2}} dx \quad (37)$$

where $d(\tau)$ is aircraft flight range calculated by mean ground speed \bar{v}_{GS} from time τ_0 to τ . Given longitude x , latitude y can be calculated by function π . As the result, aircraft 4D trajectory (x, y, h, τ) is achieved.

5. TRAJECTORY ESTIMATION SIMULATION CASE

This paper takes A319 as an example to discuss the flight trajectory estimation for flight from Chengdu shuangliu airport (ZUUU) to Xi'an xianyang airport (ZLXY). According to the flight plan, the take-off weight is 60,000 tons, the cruising airspeed is 873 km/h, and the cruising altitude is 9,500 meters.

First, assume that the standard instrument departure is JTG-01D, reduce power setting during climb, after departure enters G212 airway, whose critical points include: JTG:VOR (N30 52.4E104 23.5)-VENON (N31 04.2E104 42.2) -SUBUL (N32 19.7E106 42.6) -NSH:VOR (N33 19.4 E10818.7). The standard instrument arrival route is NSH-04A.

Then, assume the meteorological condition is ISA, wind calm, QNH is 1013.2hPa along the airway. Through the base of aircraft data (BADA), some important performance parameters are listed in Table 1.

Finally, substituting these parameters into the related model and simulating time step $\Delta\tau = 10$ s , the

horizontal trajectory which takes the airport reference point of ZUUU as reference and altitude profile are listed in Figure 5.

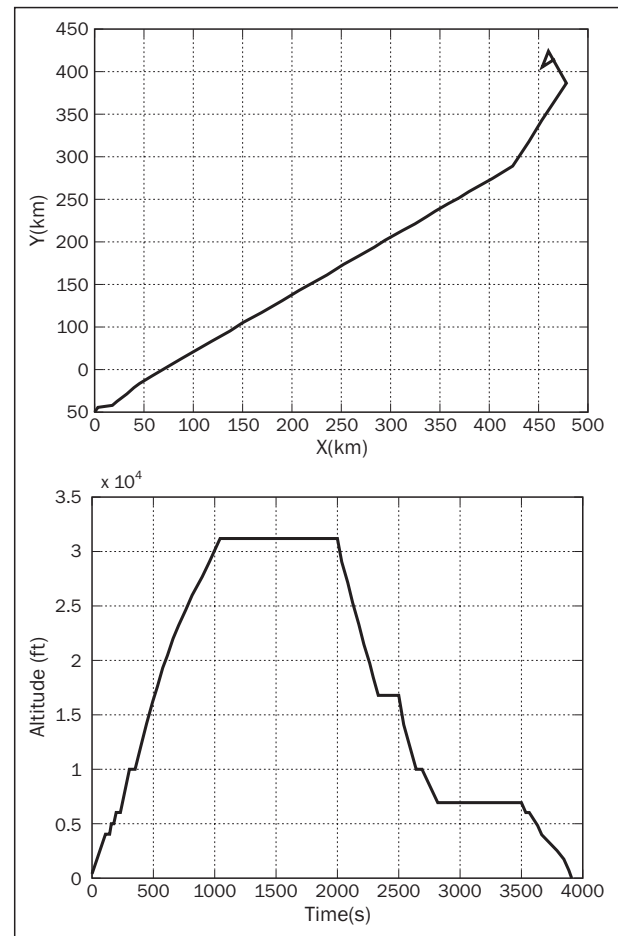


Figure 5 - Aircraft horizontal trajectory and altitude profile

According to simulation result, some critical points in estimated trajectory including the airport reference points of departure and destination airports, heading changing points, import position reporting points are completely correct. The indicator airspeed changing points, point of climb ending and point of descent satisfy the needs of the planned altitude profile.

Additionally, assuming that the airway air temperature has been changed into ISA+10, the range and altitude differential values compared with ISA in the climb phase are listed in Figure 6.

Table 1 - important parameters table in aircraft dynamic model

$C_{Tc,1}$	$C_{Tc,2}$	$C_{Tc,3}$	$C_{Tc,4}$	$C_{Tc,5}$	C_{Tcr}	C_{Tdes}^{high}	C_{Tdes}^{low}
0.14072E+06	0.47489E+05	0.96625E-10	0.94815E+01	0.94754E-02	0.95	0.83084E-01	0.51765E-01
$C_{Tdes}^{approach}$	$C_{Tdes}^{landing}$	C_{D0}^{cruise}	C_{D2}^{cruise}	$C_{D0}^{approach}$	$C_{D2}^{approach}$	$C_{D0}^{landing}$	C_{D0}^{gear}
0.14767	0.34217	0.25954E-01	0.25882E-01	0.46986E-01	0.35779E-01	0.97256E-01	0.25680E-01
$C_{D2}^{landing}$	C_{f1}	C_{f2}	C_{f3}	C_{f4}	C_{fcr}		
0.36689E-01	0.72891	0.17298E+04	0.11114E+02	0.13385E+06	0.99224		

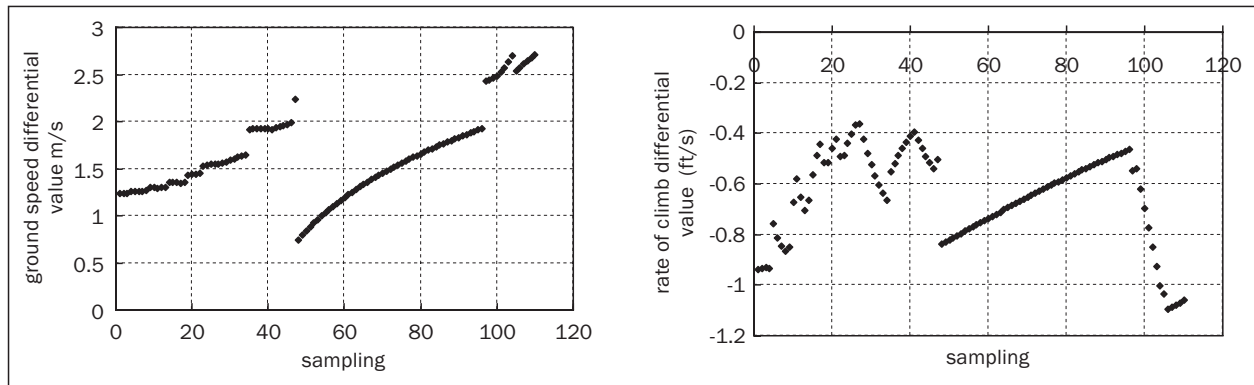


Figure 6 - Ground speed and rate of climb differential values compared with ISA

According to the compared result, when air temperature rises, the mean ground speed will increase and the time required will decrease under the same speed profiles, which coincide with the trend of aircraft performance. Additionally, the rate of climb and descent will change for the rising of air temperature, but the altitudes of critical points still satisfy the needs of planned flight altitude profile.

6. CONCLUSION

In this paper, a hybrid system model that switches the aircraft from one flight stage to another with aircraft state changing continuously in one state is proposed. The hybrid system evolution simulation is used to estimate aircraft 4D trajectory. Case study proves that aircraft 4D trajectory estimated through hybrid system model can image the changes of flight trace and altitude profile of aircraft. Further research will be focused on a combination of multiple aircraft hybrid system model for future conflict detection and resolution.

ACKNOWLEDGMENT

This work was supported by the National Science Foundation of China 61174180, by Jiangsu Province Science Foundation BK2010502 and by NUA A Research Funding NS2010177.

汤新民，南京航空航天大学副教授
中国江苏省南京市白下区御道街29号科学馆301
韩云祥，南京航空航天大学博士研究生

基于混杂系统理论的空管自动化系统4D航迹推测研究

为实现对未来大流量、高密度、小间隔条件下空域实施管理，4D航迹推测是我国新一代空管自动化系统的一项最为核心技术。本文研究在给定飞行剖面不同飞行阶段不同机型性能差异的航空器动力学模型，构造了在不同飞行阶段之间状态切换转移，而在同一阶段航空器重量、校正空速、高度和距离等状态连续变化的混杂系统模型。在此基础上通过温度和风速风向修正航空器真空速及地速，利

用混杂系统递推仿真的方式求解航空器4D航迹。实际算例表明，本文提出的混杂系统模型推测得到的水平航迹和垂直剖面能够比较准确地反映航空器的飞行状态变化和满足计划的飞行剖面的要求。

空中交通管理；4D航迹推测；混杂系统模型；航空器动力学模型

LITERATURE

- [1] Harry, S., Richard, B., Michael L.: *Next Generation Air Transportation System (NGATS) Air Traffic Management (ATM) - Airspace Project*, Reference Material, NASA, 2006
- [2] Olaf, D., Thorsten, A., Cristiano, B.: *SESAR D3 ATM Target Concept*, EUROCONTROL, 2007
- [3] Lv, X.P.: *General Framework of China's New-generation Civil Aviation ATM System*, China civil aviation, Vol.80, No.8, 2007, pp. 80: 24-26
- [4] Anthony, W.: *Trajectory Prediction Concepts for Next Generation Air Traffic Management*, 3rd USA/Europe Air Traffic Management R&D Seminar, Napoli, 2000
- [5] Yi, Q.: *Concepts of US New-generation ATM System*. China civil aviation, Vol.80, No.8, 2007, pp.80: 27-31.
- [6] Wu, K., Pan, W.: *4-D trajectory prediction model based on data mining*, Computer Applications, Vol.27, No.11, 2007, 27(11):pp. 2637-2639
- [7] Rhonda, S., Zhao Y.Y.: *Trajectory synthesis for air traffic automation*, Journal of Guidance, Control and Dynamics, Vol.20, No.2, 1997, pp.232-238
- [8] Richard, A. C.: *Climb trajectory prediction enhancement using airline flight planning information*, Proceedings of the AIAA Guidance, Navigation, and Control Conference. AIAA, 1999
- [9] Lee, H. P., Leffer, M. F.: *Development of the L-1011 four-dimensional flight management system*, NASA, 1984
- [10] Wu, S.F., Guo. S.F.: *Synthesis of aircraft vertical flight profile based on four-dimensional guidance in terminal airspace*, Acta Aeronautica ET Astronautica Sinica, Vol.14, No.5, 1993, pp. 261- 258
- [11] Wang, C., Guo. J.X., Shen. Z.P.: *Prediction of 4D Trajectory Based on Basic Flight Models*, Journal of southwest jiaotong university, Vol.44, No.2, 2009, pp. 295-300
- [12] Chester, G., William N. C.: *Using Flight Manual Data to Derive Aero-propulsive Models for Predicting Aircraft*

- Trajectories*[J]. AIAA' Aircraft Technology, Integration, and Operations(ATIO) 2002 Technical, California, 2002
- [13] Eurocontrol Experimental Centre. *User Manual for The Base of Aircraft Data*, EUROCONTROL, 2010